



# Formation of transition metal–doxorubicin complexes inside liposomes

Sheela Ann Abraham<sup>a,b,\*</sup>, Katarina Edwards<sup>c</sup>, Göran Karlsson<sup>c</sup>, Scott MacIntosh<sup>d</sup>,  
Lawrence D. Mayer<sup>a,e,f</sup>, Cheryl McKenzie<sup>a</sup>, Marcel B. Bally<sup>a,b,f</sup>

<sup>a</sup>Division of Medical Oncology, Department of Advanced Therapeutics, BC Cancer Agency, 601 West 10th Ave., Vancouver, BC, Canada V5Z 1L3

<sup>b</sup>Department of Pathology and Laboratory Medicine, Faculty of Medicine, University of British Columbia, Vancouver, BC, Canada

<sup>c</sup>Department of Physical Chemistry, Uppsala University, Uppsala, Sweden

<sup>d</sup>Department of Biochemistry and Molecular Biology, Faculty of Medicine, University of British Columbia, Vancouver, BC, Canada

<sup>e</sup>Pharmaceutical Sciences Department, University of British Columbia, Vancouver, BC, Canada

<sup>f</sup>Celator Technologies Incorporated, Vancouver, BC, Canada

Received 15 February 2002; received in revised form 25 June 2002; accepted 27 June 2002

## Abstract

Doxorubicin complexation with the transition metal manganese ( $Mn^{2+}$ ) has been characterized, differentiating between the formation of a doxorubicin–metal complex and doxorubicin fibrous-bundle aggregates typically generated following ion gradient-based loading procedures that rely on liposome encapsulated citrate or sulfate salts. The physical and chemical characteristics of the encapsulated drug were assessed using cryo-electron microscopy, circular dichroism (CD) and absorbance spectrophotometric analysis. In addition, *in vitro* and *in vivo* drug loading and release characteristics of the liposomal formulations were investigated. Finally, the internal pH after drug loading was measured with the aim of linking formation of the  $Mn^{2+}$  complex to the presence or absence of a transmembrane pH gradient. Doxorubicin was encapsulated into either 1,2-dimyristoyl-*sn*-glycero-3-phosphocholine (DMPC)/cholesterol (Chol) or 1,2-distearoyl-*sn*-glycero-3-phosphocholine (DSPC)/Chol liposomes, where the entrapped salts were citrate,  $MnSO_4$  or  $MnCl_2$ . In response to a pH gradient or a  $Mn^{2+}$  ion gradient, doxorubicin accumulated inside to achieve a drug-to-lipid ratio of approximately 0.2:1 (wt/wt). Absorbance and CD spectra of doxorubicin in the presence of  $Mn^{2+}$  suggested that there are two distinct structures captured within the liposomes. In the absence of added ionophore A23187, drug loading is initiated on the basis of an established pH gradient; however, efficient drug uptake is not dependent on maintenance of the pH gradient. Drug release from DMPC/Chol is comparable regardless of whether doxorubicin is entrapped as a citrate-based aggregate or a  $Mn^{2+}$  complex. However, *in vivo* drug release from DSPC/Chol liposomes indicate less than 5% or greater than 50% drug loss over a 24-h time course when the drug was encapsulated as an aggregate or a  $Mn^{2+}$  complex, respectively. These studies define a method for entrapping drugs possessing coordination sites capable of complexing transition metals and suggest that drug release is dependent on lipid composition, internal pH, as well as the nature of the crystalline precipitate, which forms following encapsulation.

© 2002 Elsevier Science B.V. All rights reserved.

**Keywords:** Doxorubicin; Transition metal; Ion-gradient; Liposome; Drug release

**Abbreviations:** aq, aqueous;  $Cl^-$ , chloride; Chol, cholesterol;  $^3H$ -CHE, [ $^3H$ ]-cholesteryl hexadecyl ether; CD, circular dichroism; cTEM, cryo-transmission electron microscopy;  $\Delta\epsilon$  ( $M^{-1} cm^{-1}$ ), differential molar circular dichroic absorption; DMPC, 1,2-dimyristoyl-*sn*-glycero-3-phosphocholine; DOX, doxorubicin;  $\Delta\psi$ , electrochemical gradient; EDTA, ethylenediamine-tetraacetic acid; HEPES, *N*-[2-hydroxyethyl] piperazine-*N'*-[2-ethanesulfonic acid]; HBS, HEPES-buffered saline; *i.v.*, intravenous;  $Mn^{2+}$ , manganese divalent cation; MLV, multilamellar vesicle;  $T_c$ , phase transition temperature;  $K^+$ , potassium;  $H^+$ , proton; SDS, sodium dodecyl sulfate; SHE, sucrose–HEPES–EDTA;  $MnSO_4$ , manganese sulfate solution; wt, weight; UV, ultraviolet; VIS, visible light

\* Corresponding author. Division of Medical Oncology, Department of Advanced Therapeutics, BC Cancer Agency, 601 West 10th Ave., Vancouver, BC, Canada V5Z 1L3. Tel.: +1-604-877-6098x3051; fax: +1-604-877-6011.

E-mail address: [shabraham@bccancer.bc.ca](mailto:shabraham@bccancer.bc.ca) (S.A. Abraham).

## 1. Introduction

Liposomes as model closed membrane systems have proven to be a valuable tool to characterize and define the functional roles of lipids. Liposomes have facilitated studies on lipid mobility, lipid phase behaviour and membrane permeability. The latter studies were especially insightful in terms of resolving solute permeability [1], ion gradient formation [2] and formation and stability of transmembrane electrochemical potentials [3]. An example of how these biochemical and biophysical assessments helped to define liposomes as drug carriers is illustrated by the observations of Nichols and Deamer [4], who demonstrated that liposomal systems possessing an acidic interior had the ability

to sequester catecholamines. Their studies were focused on possible mechanisms of catecholamine storage in secretory organelles but their results had far reaching effects. As first noted by Bally et al. [5], the accumulation of hydrophobic cations and lipophilic weak bases provided an important method for loading therapeutic agents into preformed membrane-bound vesicles.

Encapsulation procedures that have been developed for amphipathic drugs with protonizable amine functions involve the addition of drug to preformed liposomes possessing a pH gradient or an ion gradient capable of generating a pH gradient [6,7]. Encapsulation relies on the neutral form of the drug penetrating through the lipid bilayer, where the drug then encounters an acidic environment. The drug becomes protonated, charged and thus is retained within the liposome interior [8,9]. As more of the neutral form of the drug enters the liposome and is protonated, the amount of the neutral form on the exterior of liposomes will be depleted as the drug equilibrates across the membrane according to the Henderson–Hasselbalch equation. Protons ( $H^+$ ) are (relative to other cations) highly permeable across the lipid bilayer and will diffuse outward creating an electrochemical gradient [10] but this process will cease at a certain point due to the presence of this electrochemical gradient ( $\Delta\Psi$  negative inside). Alternatively, an electrochemical gradient can promote pH gradient formation [3]. For example, when liposomes are prepared in a potassium ( $K^+$ )-based buffer (pH 7.4) and the external solution is replaced with a buffered (pH 7.4) NaCl solution, addition of the  $K^+$  ionophore valinomycin shuttles  $K^+$  outside the liposome, creating an 150 mV electrochemical gradient ( $\Delta\Psi$ , interior negative) [10]. Protons ( $H^+$ ) readily cross the lipid bilayer into the interior, in response to the  $\Delta\Psi$  gradient and a pH gradient is thus established.

By virtue of being able to exchange selected cations, other ionophores can also establish pH gradients. Several researchers [5,11–13] have used nigericin ( $K^+$ ) ionophore and A23187 (divalent cation ionophore) to exchange specific cations for either one or two protons, respectively. When liposomes possessing a transmembrane salt gradient are incubated with the specific ionophore, the ionophores are able to facilitate the outward movement of cations for the inward movement of hydrogen ions, thereby creating a pH gradient. Regardless of the method used to generate the pH gradient, the extent of drug loading and the stability of the resulting drug loaded preparation are dependent on several factors, including drug-to-lipid ratios, entrapped buffer composition and membrane lipid composition. These factors are thought to be associated with maintenance of the pH gradient following drug loading and following in vivo administration.

It is known that gradient-based trapping procedures can result in entrapped drug levels that greatly exceed those predicted on the basis of an equilibrium established in accordance to the measured proton gradient. This is exemplified by the anthracycline doxorubicin. It has been argued that the higher than predicted drug levels can be accounted for

by calculations that consider drug membrane partitioning [14]. The more generally accepted explanation is based on the formation of an insoluble drug precipitate [15–18]. Cryo-transmission electron microscopy (cTEM) reveals doxorubicin precipitates as fibrous-bundle aggregates in both citrate and sulfate-containing liposomes [15,17]. Recently, certain researchers have suggested that the physical state of doxorubicin may also play a role in drug release [18]. It is argued here that attempts to use ion gradient-based procedures to prepare drug-loaded liposomes exhibiting optimized drug pay-out characteristics have been stymied, in part, by our lack of understanding of the physical and chemical characteristics of the encapsulated drug. For this reason, studies evaluating the role of doxorubicin precipitation in controlling the rate of drug release in vivo have been conducted. Our investigation differentiates between a drug loading method that results in formation of a transition metal–doxorubicin complex as compared to either citrate- or sulfate-based fibrous aggregates, and suggests that drug release from liposomes is dependent on a combination of internal pH, membrane lipid composition as well as the nature of the drug precipitate.

## 2. Materials and methods

### 2.1. Materials

Doxorubicin hydrochloride for injection (Faulding Quebec, Canada) was purchased from the BC Cancer Agency. 1,2-Dimyristoyl-*sn*-glycero-3-phosphocholine (DMPC) and 1,2 distearoyl-*sn*-glycero-3-phosphocholine (DSPC) was obtained from Northern Lipids Incorporated (Vancouver, BC, Canada). Cholesterol (Chol), the A23187, Sephadex G-50 and all other chemicals were obtained from the Sigma Chemical Company (St. Louis, MO, USA). [ $^3H$ ]-cholesteryl hexadecyl ether ( $^3H$ -CHE) was obtained from NEN Life Science Products, (Boston, MA, USA) and  $^{14}C$ -methylamine hydrochloride from Amersham Pharmacia Biotech. (Oakville, Canada). Pico-Fluor15 and 40 scintillation fluid was purchased from Canberra-Packard (Meriden, CT). CD-1 mice (8–10 weeks of age) were obtained from Charles River Laboratories (St. Constant, Quebec, Canada). Fetal bovine serum was bought from Hyclone Laboratories (Logan, UT).

### 2.2. Methods: preparation of liposomes

All liposomes were made from either DMPC/Chol (55:45) mole per mole (mol/mol) or DSPC/Chol (55:45) (mol/mol) and were prepared by extrusion methods. Lipids, at the indicated ratios, were dissolved in chloroform, and the  $^3H$ -CHE was added to achieve approximately 10  $\mu Ci/100$  mg lipid. The chloroform was removed under a gentle stream of nitrogen gas and, subsequently, the lipid samples were placed under a high vacuum for a time period of at

least 4 h to remove any residual solvent. The dried samples were hydrated (such that the final lipid concentration was approximately 100 mg/ml) with 300 mM citrate buffer, 300 mM  $\text{MnSO}_4$  or 300 mM  $\text{MnCl}_2$ ; adjusted to pH 3.5 by addition of hydrochloric acid. Following hydration, the multilamellar vesicles (MLVs) were subjected to five freeze-and-thaw cycles (freezing in liquid nitrogen and thawing at 40°C). The resulting frozen and thawed MLVs were prepared to optimize the salt distribution across the lipid bilayers [19]. The MLVs were extruded 10 times through stacked polycarbonate filters of 0.1 and 0.08  $\mu\text{m}$  pore size at 40°C using a water-jacketed Extruder<sup>TM</sup> (Northern Lipids). The mean size distribution of all liposome preparations was determined using a Nicomp Submicron Particle Sizer Model 270 (Pacific Scientific, Santa Barbara, CA) operating at 632.8 nm. The resulting liposome preparations typically exhibited an average diameter of approximately 100–120 nm. All liposomes, except those used for cTEM analysis and circular dichroism (CD) studies were radiolabeled. For these experiments, the phospholipid was quantitated using the Fiske and Subbarow [20] phosphate assay. Briefly, 700  $\mu\text{l}$  of 70% perchloric acid was added to lipid samples and heated to approximately 180–200°C for 2 h until the samples were colourless. Samples were cooled and 700  $\mu\text{l}$  of Fiske reagent and 7 ml of ammonium molybdate was added and samples were subsequently reheated again to 100°C for 20 min. Samples were cooled to room temperature and the absorbance was read at 820 nm.

### 2.3. Preparation of ion gradients for doxorubicin encapsulation

Large unilamellar liposomes in the indicated buffers were fractionated on Sephadex G-50 columns (1 ml sample volumes were placed on columns with at least a 20 ml column bed) equilibrated with various buffers at pH 7.5. The buffers used for the external environment included 25 mM HEPES/150 mM NaCl (HBS) for the liposomes with encapsulated 300 mM citrate and 300 mM sucrose/20 mM HEPES/15 mM EDTA (SHE) for the liposomes with encapsulated  $\text{MnSO}_4$  and  $\text{MnCl}_2$ . The manganese sulfate-based procedure for doxorubicin loading was a modification of the method described by Cheung et al. [11]. In particular, it should be noted that the solubility of 300 mM  $\text{MnSO}_4$  is highly variable under the pH conditions described in the original procedure, presumably resulting in the formation of  $\text{Mn}(\text{OH})_2(\text{s})$ . In the studies reported here, liposomes were prepared in a 300 mM  $\text{MnSO}_4$  (and  $\text{MnCl}_2$ ) solution at a pH of 3.5; solutions that are stable for months at room temperature.

### 2.4. Drug loading and release

Following formation of the salt gradients as described above, the liposome lipid concentration was adjusted to 10 mg/ml and, subsequently, doxorubicin was added to

achieve a drug-to-lipid ratio (wt/wt) of 0.2:1 at 20, 40 and 60°C. The accumulation of doxorubicin into liposomes was determined at the indicated time points by removing 100  $\mu\text{l}$  aliquots and separating unencapsulated drug from encapsulated drug on 1 ml Sephadex G-50 (medium) spin columns equilibrated with the appropriate buffer. The concentration of doxorubicin in the excluded fraction was determined by measuring absorbance (at 480 nm) of a solution consisting of the sample, adjusted to 100  $\mu\text{l}$  with HBS or SHE, to which 900  $\mu\text{l}$  of 1% Triton X-100 was added. Prior to assessing absorbance at 480 nm, the sample was placed in >90°C water bath until the cloud point of the detergent was observed. Liposome lipid concentrations were determined by adding a small aliquot of the excluded fraction to 5 ml of scintillation cocktail, where the radioactivity of the sample was subsequently determined by scintillation counting with the Packard 1900TR Liquid Scintillation Analyzer.

The *in vitro* doxorubicin release assay used liposomes with a drug-to-lipid ratio of 0.2:1 (wt/wt). Samples were mixed with fetal bovine serum such that the final lipid concentration was 2 mg/ml and the final serum concentration was 50%. These samples were incubated at 37°C and at the indicated time-points, 100  $\mu\text{l}$  aliquots were placed onto 1 ml spin columns. The liposome lipid concentration was quantitated via liquid scintillation techniques and encapsulated doxorubicin was assayed as described above.

For the *in vivo* studies assessing doxorubicin release, drug-loaded liposomes (0.2:1 drug-to-lipid ratio, wt/wt) were adjusted to a lipid concentration required to administer a 100 mg/kg liposomal lipid or 20 mg/kg doxorubicin dose in an injection volume of 200  $\mu\text{l}$ . This dose translates to approximately 45.7  $\mu\text{mol Mn}^{2+}/\text{kg}$  of for DMPC–Chol liposomes or 40.95  $\mu\text{mol Mn}^{2+}/\text{kg}$  for DSPC–Chol liposomes, which are well below the acute  $\text{LD}_{50}$  value of 272  $\mu\text{mol Mn}^{2+}/\text{kg}$  (95% confidence limits: 227–326  $\mu\text{mol Mn}^{2+}/\text{kg}$ ) [21] determined for mice. Various formulations were injected intravenously (*i.v.*, via the lateral tail vein) into 20–22 g female CD-1 mice. At 1, 4 and 24 h after injection, the animals were terminated by  $\text{CO}_2$  asphyxiation and blood was collected by cardiac puncture and placed into EDTA coated microtainers. Plasma was prepared by centrifuging the blood samples at  $\sim 500 \times g$  for 10 min. Plasma was removed carefully such that the buffy coat was not disturbed and collected into Eppendorf tubes. The plasma lipid concentrations were measured on the basis of the incorporated  $^3\text{H}$ -CHE marker, which is nonexchangeable and nonmetabolizable [22]. Samples of 50–100  $\mu\text{l}$  were mixed with 5 ml of PicoFluor-40 scintillation cocktail prior to assessing the radioactivity.

Plasma doxorubicin levels were determined following extraction of the drug from plasma using a procedure involving addition of 800  $\mu\text{l}$  of 10% SDS and 10 mM  $\text{H}_2\text{SO}_4$  to a plasma sample diluted to 200  $\mu\text{l}$  in HBS or SHE. These samples were briefly vortexed prior to addition of 2 ml of a 1:1 isopropanol–chloroform mixture. This sample

was again vortexed vigorously prior to freezing in a  $-80^{\circ}\text{C}$  freezer for at least 4 h to help precipitate out plasma proteins. The samples were thawed to room temperature and then centrifuged at  $2000 \times g$  for 15 min to separate the organic layer (bottom layer that contains doxorubicin) from the aqueous layer and protein interface. The amount of doxorubicin associated fluorescence in the organic phase was determined using a Perkin Elmer LS50B luminescence spectrometer using an excitation wavelength of 470 nm (slit width=2.5) and an emission wavelength of 550 nm (slit width=10). The fluorescence readings were compared to a standard curve of doxorubicin, which was prepared using known amounts of doxorubicin that were extracted into an organic phase using the identical procedure used for the unknowns.

All animal studies were done according to procedures approved by the University of British Columbia Animal Care Committee. These studies meet the requirements outlined in the current guidelines for animal use established by the Canadian Council of Animal Care.

To assess the stability of doxorubicin within the manganese-containing liposomes and confirm that manganese is not inducing doxorubicin degradation, high-performance liquid chromatography (HPLC) was used to resolve intact doxorubicin. Drug-loaded liposomes (0.2:1 drug-to-lipid ratio, wt/wt) were incubated and at the indicated time-points, 100  $\mu\text{l}$  aliquots were placed onto 1 ml spin columns. The liposome lipid concentration was quantitated via liquid scintillation techniques and encapsulated doxorubicin was assayed using HPLC. HPLC was done using a Waters Alliance 2690 HPLC system with Waters 474 Fluorescence Detector set at an excitation wavelength of 480 nm and emission wavelength of 580 nm, controlled by Waters Millennium 32 software. Fifty microlitres of sample was injected onto a Waters Symmetry C18 column,  $4.6 \times 75$  mm using a mobile phase of 78% 16 mM ammonium formate buffer pH 3.5, 15% acetone and 7% isopropanol at 1 ml/min. Column temperature was maintained at  $40^{\circ}\text{C}$  and samples at  $5^{\circ}\text{C}$ .

### 2.5. pH gradient determination

Transmembrane pH gradients were monitored employing [ $^{14}\text{C}$ ]-methylamine. Briefly, [ $^{14}\text{C}$ ]-methylamine (0.5  $\mu\text{Ci/ml}$ ) was added to a liposome solution containing  $< 10$  mg/ml of lipid. After 15 min, 150  $\mu\text{l}$  aliquots were passed down 1 ml Sephadex G-50 columns at  $60^{\circ}\text{C}$  equilibrated in HBS to remove unencapsulated methylamine (column run time of 3–5 min). Lipid and methylamine concentrations before and after column chromatography were determined by scintillation counting. The transmembrane pH gradient was then calculated according to the relationship:

$$\Delta\text{pH} = \log\left\{\frac{[\text{H}^+]_{\text{inside}}}{[\text{H}^+]_{\text{outside}}}\right\} \\ = \log\left\{\frac{[\text{methylamine}]_{\text{inside}}}{[\text{methylamine}]_{\text{outside}}}\right\}$$

It should be noted that under the conditions employed, the exterior pH did not change during the uptake process.

### 2.6. Absorption and CD spectra

To verify if manganese was indeed binding to doxorubicin, changes in doxorubicin absorption spectra under various proton and metal concentrations was determined using a Hewlett Packard 8453 UV–Visible Spectroscopy System (cell path length=1.00 cm). Doxorubicin was added to buffers at pH 6 (100 mM MES), pH 8 (100 mM HEPES), pH 9 (100 mM CHES), pH 10 (100 mM CAPS), pH 11 (100 mM CAPS) and pH 13 (100 mM glycine + 100 mM NaCl) at a constant doxorubicin concentration of 86  $\mu\text{M}$ . At the concentrations used  $\text{MnSO}_4$ ,  $\text{MnSO}_4$  had a very low solubility in basic solutions. In order to circumvent this problem,  $\text{MnSO}_4$  (s) was added to buffered solutions containing 100 mM HEPES at pH 8 and vigorously vortexed. Due to the formation of  $\text{Mn}(\text{OH})_2$  precipitate (within 12 h), absorbance readings were done immediately, well before the visible formation of the precipitate. To monitor electronic state changes within doxorubicin-loaded liposomes, CD spectra of each drug loaded liposome preparation were analysed. CD measurements were obtained using the Jasco J-720 spectropolarimeter, which was calibrated using 0.06% (w/v) ammonium-D-10-camphorsulfonate. All spectra were recorded using a 0.1 cm cell and the following parameters:  $\lambda=220\text{--}750$  nm, step resolution=1 nm, speed=20 nm/min, response=0.25 s, band width=1.0 nm. Results are expressed in differential molar CD absorption  $\Delta\epsilon$  ( $\text{M}^{-1} \text{cm}^{-1}$ ),

$$\Delta\epsilon = \theta/32980 \times C \times l$$

where  $\theta$ =molar ellipticity,  $C$ =molar concentration, and  $l$ =path length of cell in centimeters.

### 2.7. Cryo-transmission electron microscopy

DMPC/Chol liposomes were prepared as described above without the  $^3\text{H}$ -CHE lipid marker. Liposomes were loaded with doxorubicin at a 0.2:1 drug-to-lipid ratio (wt/wt). In a chamber of controlled temperature ( $25^{\circ}\text{C}$ ) and humidity, 1–2  $\mu\text{l}$  of liposome sample (before or after the addition of drug) was added and blotted onto copper grids coated with a cellulose acetate butyrate polymer. The samples were quickly vitrified by plunging into liquid ethane and transferred to liquid nitrogen keeping the sample below 108 K, therefore minimizing sample perturbation and the formation of ice crystals. The grid was transferred to a Zeiss EM902 transmission electron microscope where observations were made in a zero-loss bright-field mode and an accelerating voltage=80 kV.

### 3. Results

#### 3.1. The encapsulation of doxorubicin into DMPC/Chol liposomes using the citrate loading procedure or the manganese sulfate loading procedure

The first objective of this study was to compare the manganese sulfate loading procedure [11,13] to the citrate-based loading method, using doxorubicin as a model drug. The citrate loading procedure relies on an established pH gradient across the liposome bilayer and the use of encapsulated 300 mM citrate as a buffer to minimize changes in interior pH as doxorubicin redistributes across the liposomal membrane according to the transmembrane gradient (interior acidic) (see Fig. 1A). It should be noted that when doxorubicin is encapsulated using this method, the resulting drug-loaded liposomes appear as a bright opaque orange colour. When doxorubicin is encapsulated using the manganese sulfate-based loading procedure described by Cheung et al. [11] (Fig. 1B,C), a pH and a metal ion

gradient are present across the liposome. Similar to the citrate-based loading method doxorubicin, it is anticipated that the neutral form of the drug crosses the lipid bilayer. Subsequently, the amine group becomes protonated, resulting in an increase in the liposomes' interior pH. In order to maintain the interior pH, other researchers [11] have used the divalent cation ionophore A23187 (an electro-neutral ionophore capable of translocating a divalent cation for the exchange of two hydrogen ions). A23187 shuttles protons to the vesicle interior in exchange for  $Mn^{2+}$  ions [23], which are subsequently chelated by EDTA contained in the exterior buffer (Fig. 1C). The opaque orange colour of the resulting drug loaded liposomes is visually comparable to solutions prepared using the citrate-based loading method and free doxorubicin at pH 3–7. Perhaps most interestingly, in the absence of the ionophore (Fig. 1B), doxorubicin loading is accompanied by a change in the colour of the solution from orange to an opaque royal purple colour.

To compare the three different loading methods described in Fig. 1, the accumulation of doxorubicin into DMPC/Chol liposomes was determined as a function of temperature and time. The drug loading parameters were determined under conditions where the drug and liposomes were mixed at a drug-to-lipid ratio (wt/wt) of 0.2:1 and the final liposome lipid concentration was adjusted to 10 mM for each method. The doxorubicin loading data, summarized in Fig. 2, indicate that the loading attributes for all three methods are comparable at all temperatures evaluated. At 20°C, the drug-to-lipid ratio does not change over the entire time course, a result consistent with drug membrane partitioning but no accumulation. Optimal loading occurs when the incubation temperature is adjusted to 60°C, where >95% of the added doxorubicin is encapsulated within the liposomes within 5 min.

To assess the stability of doxorubicin within the manganese-containing liposomes and confirm that manganese is not inducing doxorubicin degradation, HPLC was used to resolve intact doxorubicin (Fig. 3). Doxorubicin loaded DMPC/Chol and DSPC/Chol liposomes (0.2:1 drug-to-lipid ratio, wt/wt), were prepared using the citrate or the manganese sulfate-based loading procedures. Changes in drug-to-lipid ratios were used to calculate the percent (%) of remaining doxorubicin, measured at various time points over a 48-h time course. In both the DMPC/Chol (Fig. 3A) and DSPC/Chol (Figure 3B) liposomes, total intact doxorubicin concentrations within citrate and manganese-containing liposomes were comparable over the time course. There was approximately a 9% greater level of intact doxorubicin in citrate as compared to the manganese loaded DMPC/Chol liposomes and a 10% greater level of intact doxorubicin in the citrate as compared to the manganese loaded DSPC/Chol liposomes at the 48 h timepoint. It is important to note that the methods described are consistent with a reconstitution procedure that involves encapsulation of the drug in preformed liposomes just prior to drug administration. This procedure

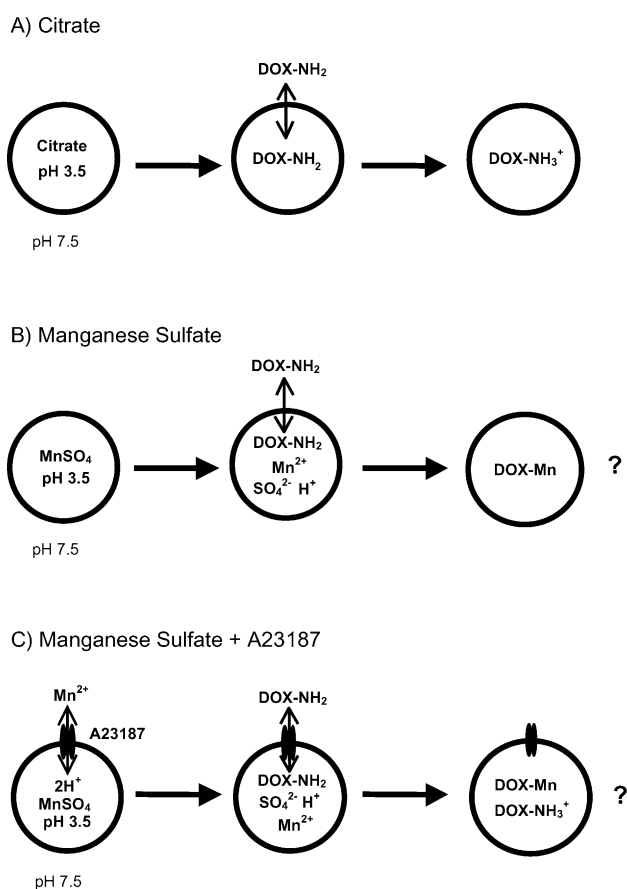


Fig. 1. Methods of doxorubicin encapsulation into liposomes exhibiting the indicated gradients: (A) liposomes prepared in 300 mM citrate buffer, pH 3.5, and outside buffer exchanged to HBS at pH 7.5, (B) liposomes prepared in 300 mM manganese sulfate, pH 3.5, and outside buffer is exchanged to 300 mM sucrose/20 mM HEPES/15 mM EDTA at pH 7.5 and (C) which is identical to (B) except that the ionophore A23187 is added to the liposomes prior to doxorubicin addition.

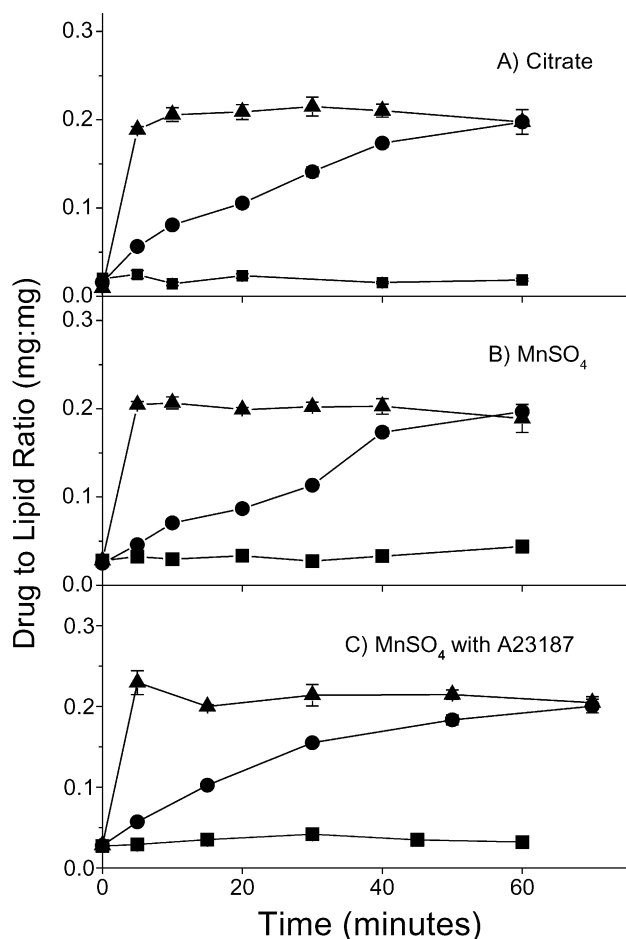


Fig. 2. Doxorubicin encapsulation in DMPC/Chol (55:45) liposomes using the three loading methods, illustrated in Fig. 1, and based on liposomes prepared using (A) citrate loading procedure, (B) the manganese sulfate loading procedure or, (C) the manganese sulfate loading procedure with the A23187 ionophore. Liposomes were prepared as described in Methods and the outer buffers were exchanged using column chromatography in order to create a pH or a  $Mn^{2+}$  gradient. For the  $MnSO_4$  loading procedure, the A23187 was added and incubated 5 min prior to the addition of drug. Doxorubicin was added to the liposomes to achieve a 0.2:1 drug-to-lipid ratio (wt/wt) and incubated at either 20°C (■), 40°C (●) or 60°C (▲). At the indicated time points, aliquots were fractionated on 1 ml spin columns to separate encapsulated drug (collected in the void volume) from unencapsulated drug. Lipid concentrations were determined using  $^3H$ -CHE and doxorubicin was quantitated by reading the  $A_{480}$  of a detergent solubilized sample as described in the Methods. Data points represent the mean drug-to-lipid ratios of at least three replicate experiments and the error bars indicate the standard deviation.

has been validated in the clinic for formulations of doxorubicin and vincristine [36].

### 3.2. Cryo-transmission electron microscopic analysis of the drug-loaded liposomes

Doxorubicin, when loaded into sulfate or citrate-containing liposomes with an acidic interior ( $pH < 5$ ), will form a precipitate, particularly when the final drug-to-lipid ratio is in excess of 0.05:1 (wt/wt) [2,15,17,18]. One of the best

methods to evaluate formation of the drug precipitate within liposomes relies on use of cTEM [2,24]. For this reason, cryo-electron micrographs of the DMPC/Chol liposomal formulations, before and after drug loading, were obtained and representative images are shown in Fig. 4. The image shown in Fig. 4IA is of liposomes prepared in a 300 mM citrate buffer (pH 3.5) after the exterior buffer was exchanged to HBS (pH 7.5). These liposomes appear to be mostly spherical and uniform in size ranging around 120 nm; a value that is consistent with the size determined by light scattering analysis (see Methods). Following accumulation of doxorubicin to a final drug-to-lipid ratio of 0.2:1 (wt/wt), a precipitate is readily visible within the vesicular structures (Fig. 4IIA). The doxorubicin bundles appear as linear or circular structures, and drug precipitation can induce a change in the shape of the liposomes, resulting in a “coffee bean” like appearance.

Liposomes prepared in 300 mM  $MnSO_4$  with the exterior buffer exchanged to the EDTA-containing pH 7.5 buffer, appear as elongated and tubular structures (Fig. 4IB,IC) in comparison to the citrate-containing liposomes (Fig. 4IA). When these liposomes are loaded with doxorubicin using A23187, the resulting liposomes have a pronounced elongated structure and what appears to be a linear bundle of

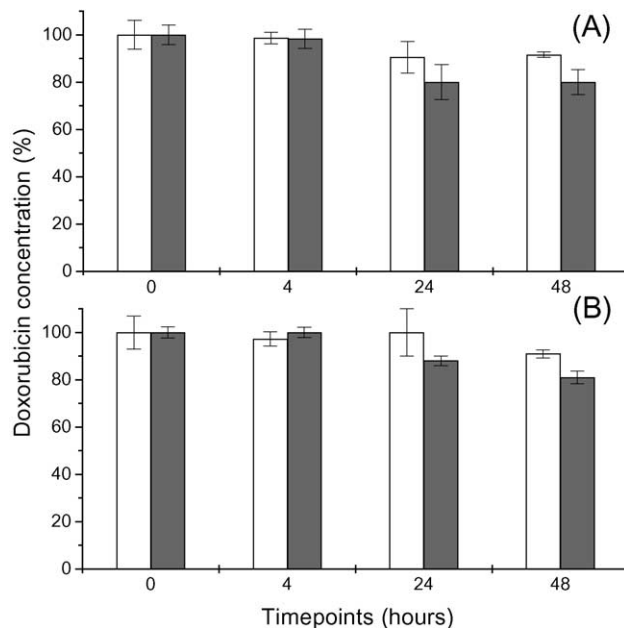


Fig. 3. The stability of doxorubicin within DMPC/Chol (55:45) and DSPC/Chol liposomes containing either citrate or manganese sulfate. DMPC/Chol (A) or DSPC/Chol (B) liposomes were loaded with doxorubicin to achieve a final drug-to-lipid ratio of 0.2:1 (wt/wt) using the citrate (white bars) or the manganese sulfate (black bars) procedures as previously described in Methods. At the indicated time points, the drug and liposomal lipid concentrations were measured after fractionating samples on a 1 ml spin column as described in the Methods. Doxorubicin was measured using HPLC to provide a measure of intact drug. These data were used to calculate the percentage of remaining doxorubicin at various time points. Data points represent the mean of data obtained from six separate experiments and the error bars indicate the standard deviation for each data point.

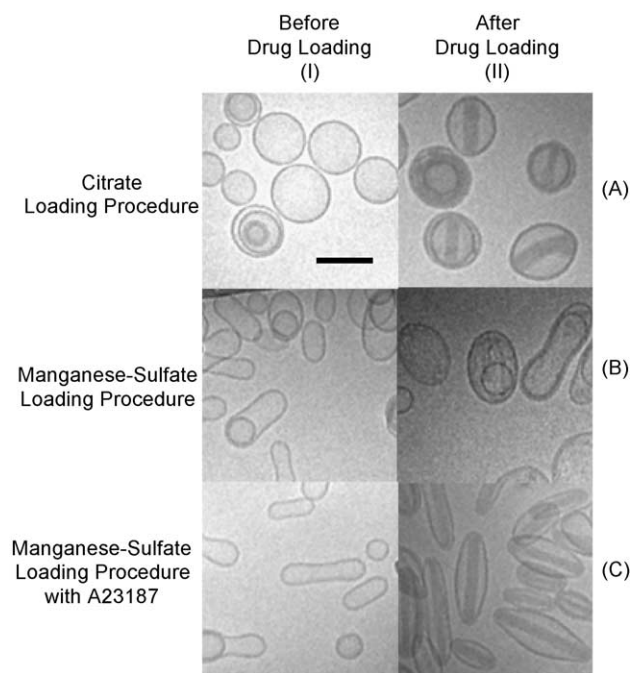


Fig. 4. cTEM images of DMPC/Chol (55:45) liposomes either before or after drug loading achieving a final drug-to-lipid ratio of 0.2:1 (wt/wt). The liposomes were prepared as described in Methods and loaded with doxorubicin as summarized in Fig. 2. Briefly, the samples were incubated at 60°C for 30 min in order to facilitate >95% doxorubicin encapsulation. cTEM images were obtained from liposome samples prior to drug addition and from liposomes with encapsulated drug. All images are representative of the entire sample. (Panel IA) DMPC/Chol liposomes prepared in 300 mM citrate, pH 3.5, and with the outside buffer changed to HEPES-buffered saline, pH 7.5, as the exterior buffer. (Panel IIA) Same as those described for IA except after liposomes have been loaded with doxorubicin. (Panel IB) DMPC/Chol liposomes prepared in 300 mM MnSO<sub>4</sub>, pH 3.5, and with the outside buffer changed to SHE, pH 7.5. (Panel IIB) Same as those described in IB except after liposomes have been loaded with doxorubicin. (Panel IC) DMPC/Chol liposomes prepared in 300 mM MnSO<sub>4</sub>, pH 3.5; with the outside buffer changed to SHE, pH 7.5, and following addition of the ionophore A23187. (Panel IIC) Same as those described in IC except after liposomes have been loaded with doxorubicin. The bar in panel IA is equivalent to 100 nm and all micrographs are shown at the same magnification.

precipitated doxorubicin within the core. In contrast, there is no obvious precipitate inside doxorubicin-loaded liposomes prepared in the absence of A23187. The cryo-electron microscopic images of these liposomes reveal a stippled and diffuse morphology within the liposome core (Fig. 4IIB). These results clearly indicate significant differences in the doxorubicin-containing liposomes prepared with and without A23187. The next series of experiments were designed to assess the role of entrapped sulfate and interior pH on the formation of the doxorubicin precipitate.

### 3.3. The encapsulation of doxorubicin into liposomes prepared in manganese chloride

In order to assess the role of the sulfate anion in mediating precipitation of doxorubicin, drug loading in liposomes with

encapsulated MnCl<sub>2</sub> was characterized. A solution of 300 mM MnCl<sub>2</sub> (pH 3.5) was used to prepare DMPC/Chol liposomes and following gradient formation (see Methods), doxorubicin was added to achieve a final drug-to-lipid ratio of 0.2:1 (wt/wt). Similar to results obtained when using entrapped MnSO<sub>4</sub> in the absence of A23187, doxorubicin loading occurred optimally at 60°C and no loading was observed at 20°C (Fig. 5A). The resulting drug-loaded liposomes were opaque royal purple in colour. Under conditions where MnCl<sub>2</sub> loaded liposomes were incubated with doxorubicin in the presence of A23187 (Fig. 5B), drug loading was also achieved at 60°C; however, the resulting liposome preparation had an orange appearance. Following drug loading to achieve the maximum 0.2:1 drug-to-lipid ratio (wt/wt), there was a time-dependent decrease in the drug-to-lipid ratio from 0.2:1 (measured at 20 min) to less than 0.15:1 (measured at 40 min).

Representative cryo-electron micrographs obtained from the MnCl<sub>2</sub> liposome formulation are shown in Fig. 6. These images suggest that in the presence or absence of A23187, the core of the drug-loaded liposomes have a stippled and diffuse precipitate (Fig. 6IIA,IIB). The results suggest that formation of the fibrous bundle, observed following A23187

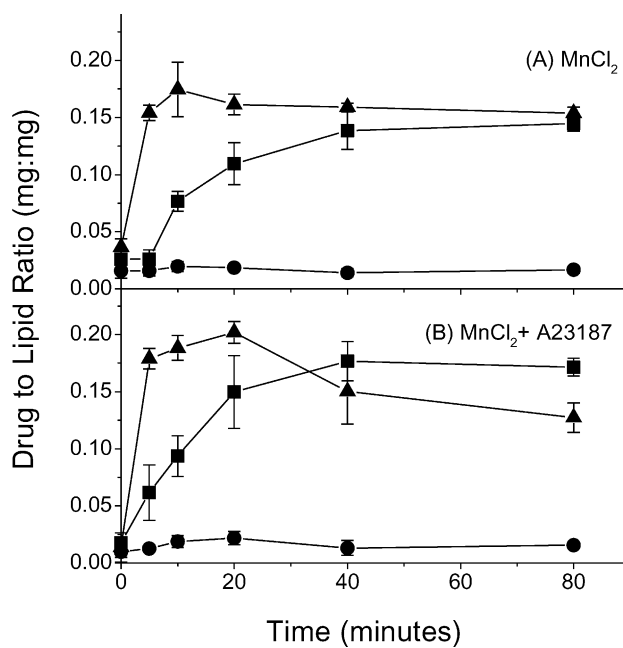


Fig. 5. Doxorubicin encapsulation using liposomes prepared in 300 mM manganese chloride, pH 3.5, and with the external buffer exchanged to SHE, pH 7.5. Drug loading was measured in the presence (B) and absence (A) of the ionophore A23187. The methods used were identical to those described for the manganese sulfate loading procedure and are summarized in the legend to Fig. 2 and Methods. Briefly, doxorubicin was added to achieve a final drug-to-lipid ratio of 0.2:1 (wt/wt). Subsequently, the samples were incubated at either 20°C (■), 40°C (●) or 60°C (▲) and at the indicated time points, the sample was passed through a 1 ml spin column to separate free drug from encapsulated, which was quantitated as described in Methods. The data points represent the mean drug-to-lipid ratios obtained from three separate experiments and the error bars indicate the standard deviation.

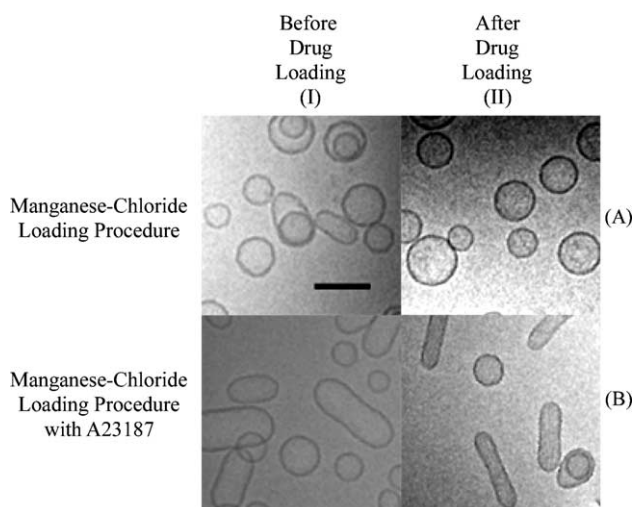


Fig. 6. cTEM images of DMPC/Chol (55:45) liposomes either before or after drug loading, achieving a final drug-to-lipid ratio of 0.2:1 (wt/wt). The liposomes were prepared as described in Methods and loaded with doxorubicin as summarized in Fig. 5. Briefly, the samples were incubated at 60°C for 30 min in order to facilitate >95% doxorubicin encapsulation. cTEM images were obtained from a liposome sample prior to drug addition and from liposomes with encapsulated drug. All images are representative of the entire sample. (Panel IA) DMPC/Chol liposomes prepared in 300 mM MnCl<sub>2</sub>, pH 3.5, and with the outside buffer changed to SHE, pH 7.5, as the exterior buffer. (Panel IIA) Same as those described for IA except after liposomes have been loaded with doxorubicin. (Panel IB) DMPC/Chol liposomes prepared in 300 mM MnCl<sub>2</sub>, pH 3.5; with the outside buffer changed to SHE, pH 7.5, and after the addition of the ionophore A23187. (Panel IIB) Same as those described in IB except after liposomes have been loaded with doxorubicin. The bar in panel IA is equivalent to 100 nm and all micrographs are shown at the same magnification.

mediated doxorubicin loading into liposomes prepared in 300 mM MnSO<sub>4</sub> was due, in part, to the presence of the sulfate anion. Osmotic gradients across liposomes influence liposome shape and it should be noted that when preparing the citrate and MnCl<sub>2</sub> (300 mM citrate (580 mOsm/l) 300 mM MnCl<sub>2</sub> (785 mOsm/l)) liposomes, there is an osmotic gradient across the membrane (exterior solutions of HBS (326 mOsm/l) and SHE (517 mOsm/l), respectively), which results in the inward movement of water. This results in a “swelling” of the liposomes and thus they appear as round structures (Figs. 4IA and 6IA). In contrast, the MnSO<sub>4</sub>-loaded liposomes are hypoosmotic (300 mM MnSO<sub>4</sub> (319 mOsm/l) and with respect to its environment SHE (517 mOsm/l)) and results in the movement of water to the outside. Thus, these liposomes appear as oblong structures (see Fig. 4IB,IC for comparison). Following addition of A23187 (with the shuttling of the divalent cations out of the liposomes) and doxorubicin loading, the liposomes become even more elongated.

### 3.4. Assessment of the transmembrane pH gradient prior to and following doxorubicin loading

One of the distinguishing features of the loading procedure that relies on encapsulated MnSO<sub>4</sub> is the absence of an

effective internal buffer. In fact, doxorubicin loading in the absence of A23187 should result in a rapid dissipation of the transmembrane pH gradient. Radiolabeled methylamine was used as a pH-sensitive probe [3,10] to measure the pH gradient across the liposomal formulations after exchanging the exterior buffers and following doxorubicin uptake. As noted in Methods, all liposomal formulations were prepared in solutions with a pH of 3.5. Thus, following the external buffer exchange, it was anticipated that the transmembrane pH gradient would be approximately four units. Three formulations were evaluated in these studies and the results have been summarized in Fig. 7. Following the establishment of the pH gradient, but prior to doxorubicin loading, the formulations with encapsulated citrate (column 1), MnSO<sub>4</sub> (column 3), and MnCl<sub>2</sub> (column 7) exhibited measured transmembrane pH gradients of 3.4, 1.6, and less than 0.18, respectively. Therefore, even in the absence of drug loading or ionophore addition, the Mn-based formulations had significantly smaller pH gradients. Following addition of doxorubicin, the pH gradient of the citrate-based formulation decreased from 3.4 (column 1) to 2.3 (column 2), a result that is consistent with previous reports demonstrating doxorubicin-mediated decreases in the pH gradient in these formulations [25].

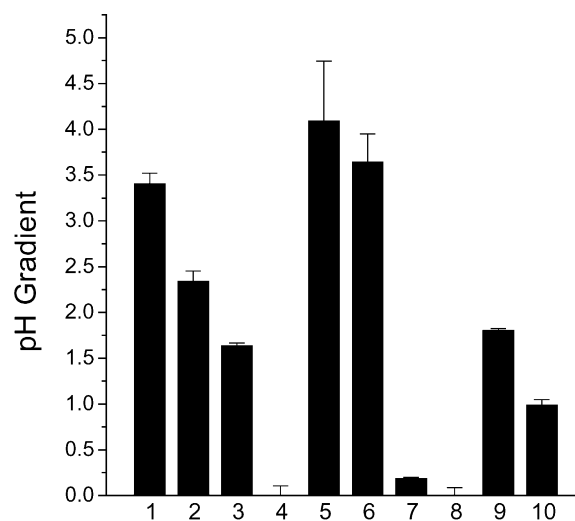


Fig. 7. Measured transmembrane pH gradients prior to and following doxorubicin loading under the various conditions as described in Figs. 2 and 5. The pH gradient was estimated through use of radiolabeled methylamine as described in Methods. Radiolabeled methylamine was added to liposomes after they were incubated at 60°C for 30 min either in the presence or absence of doxorubicin. Doxorubicin was added to achieve a final drug-to-lipid ratio of 0.2:1 (wt/wt). The samples include those based on the citrate loading method (column 1), with doxorubicin (column 2); the MnSO<sub>4</sub>-loading method (column 3), with doxorubicin (column 4). The MnSO<sub>4</sub>-loading method with A23187 (column 5), with doxorubicin (column 6); the MnCl<sub>2</sub>-loading method (column 7), with doxorubicin (column 8) and the MnCl<sub>2</sub>-loading method plus the ionophore A23187 (column 9) with doxorubicin (column 10). The results represent the mean pH gradient of three separate experiments and the error bars indicate the standard deviation.



In the absence of the ionophore, but following doxorubicin loading, the Mn-containing formulations exhibited no measurable transmembrane pH gradient (refer to Fig. 7, columns 4 and 8). This result indicates, unequivocally, that these doxorubicin-loaded preparations no longer maintain a pH gradient and this is consistent with the fact that these formulations have little or no ability to buffer against changes in pH induced by drug loading. In contrast, the addition of A23187 to either the  $\text{MnSO}_4$  (column 5) or  $\text{MnCl}_2$  (column 9) containing liposome formulations resulted in generation of a substantial pH gradient. As estimated using methylamine, these pH gradients were approximately 4.0 and 1.8, respectively. Even following doxorubicin loading, these two formulations (columns 6 and 10) maintained pH gradients of 3.6 and 1.0, respectively.

### 3.5. Absorption and CD spectra of doxorubicin under various conditions

In order to explore the role of  $\text{Mn}^{2+}$  ion complexation with doxorubicin, and the associated influence of pH, spectroscopic studies were completed. Doxorubicin (see inset to Fig. 8) possesses a chromophore with multiple  $\pi \rightarrow \pi^*$  and  $n \rightarrow \pi^*$  transitions rendering doxorubicin's electronic absorption and CD spectra sensitive to the deprotonation of the chromophore and the binding of metal ions [26,27]. As shown in Fig. 8A, when the pH increases, there is a visible bathochromic shift observed with two predominant absorption bands appearing at 550 and 590 nm. This spectral shift has been attributed to deprotonation of the hydroxyls at the C(6) ( $\text{pK}_a = 13.2$ ) and C(11) ( $\text{pK}_a = 10.16$ ) positions [27]. We observed a similar shift of the doxorubicin spectra at a fixed pH (pH 8.0) following the addition of  $\text{MnSO}_4$  (Fig. 8B). The observed bathochromic shift resulted in two predominant absorption bands centered around 542 and 581 nm. The shift was observed even in

the presence of 100 mM  $\text{MnSO}_4$ . These results suggest that in the presence of  $\text{Mn}^{2+}$ , the ion is potentially capable of deprotonating the chromophore at the C(11)-OH and C(6)-OH positions.

To further characterize the interactions of  $\text{Mn}^{2+}$  with doxorubicin, CD spectra of doxorubicin-loaded liposomes were obtained. The formulations evaluated include ones where the drug was encapsulated using the citrate-based and the manganese sulfate-based loading procedures. The latter was completed in the absence and presence of A23187. As shown in Fig. 8C, the CD spectra obtained for encapsulated doxorubicin prepared using the citrate and the  $\text{MnSO}_4$  plus A23187 loading methods were similar. This result is likely due to the similar conformations doxorubicin

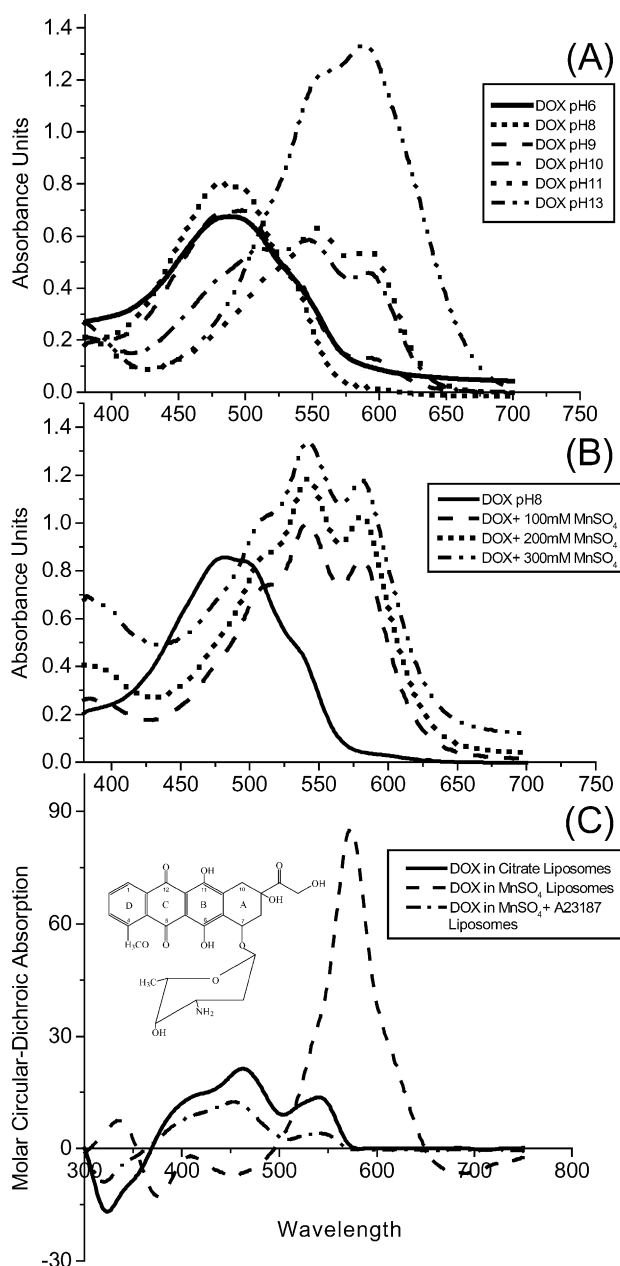


Fig. 8. Absorption spectra of doxorubicin at various pHs and concentrations of  $\text{MnSO}_4$  as well as the CD spectra of doxorubicin-loaded liposomes. (A) The absorbance spectra of an 86  $\mu\text{M}$  doxorubicin solution at pH 6, 8, 9, 10, 11, and 13. The pH of each sample was maintained by either 100 mM MES (pH 6), 100 mM HEPES (pH 8), 100 mM CHES (pH 9), 100 mM CAPS (pH 10), 100 mM CAPS (pH 11) and 100 mM glycine + 100 mM NaCl (pH 13). The absorbance spectra were obtained immediately after drug solubilization to minimize doxorubicin degradation. (B) Representative absorption spectra of an 86  $\mu\text{M}$  doxorubicin solution in the presence of various concentrations of  $\text{MnSO}_4$  at pH 8.  $\text{MnSO}_4(\text{s})$  was added to 1 ml of 100 mM HEPES at pH 8 and vigorously vortexed, then doxorubicin was added to obtain a final concentration of approximately 86  $\mu\text{M}$ . The solubility of  $\text{MnSO}_4$  at pH 8 is low and the formation of  $\text{Mn}(\text{OH})_2(\text{s})$  is a limiting factor, therefore absorbance readings were taken immediately. There was no visible precipitation in the sample within the time frame required to obtain the spectra. (C) Representative CD spectra of doxorubicin-loaded DMPC/Chol liposomes, where drug loading was achieved using either the citrate or the manganese sulfate  $\pm$  A23187 loading procedures. Empty DMPC/Chol liposomes containing either 300 mM citrate or 300 mM manganese sulfate were analysed as controls and showed  $\Delta\epsilon \sim 0$  as a function of  $\lambda = 300\text{--}800$  nm (data not shown).

Table 1  
The differential molar CD absorption  $\Delta\epsilon$  ( $M^{-1} \text{ cm}^{-1}$ ) of doxorubicin-encapsulated liposomes

Loading procedures	$\pi \rightarrow \pi^*$ (z-axis)	$n \rightarrow \pi^*$ C(12)=O	$n \rightarrow \pi^*$ C(5)=O	$\pi \rightarrow \pi^*$ (y-axis)		
	300 nm <sup>a</sup>	330 nm	346 nm	448 nm	513 nm	542 nm
Manganese sulfate ( $\Delta\epsilon$ )	-1.08	6.79	5.02	-6.84	8.60	35.20
Citrate ( $\Delta\epsilon$ )	0.062	-15.37	-9.51	18.85	10.13	13.63
Manganese sulfate ( $\Delta\epsilon$ ) with A23187	-0.94	-6.94	-3.14	12.30	2.60	4.03

Doxorubicin was loaded into liposomes using the citrate, the manganese sulfate or the manganese sulfate with A23187 procedure as described in Methods. Specific wavelengths correspond to potential electronic transitions undergone by doxorubicin following encapsulation.

<sup>a</sup> Wavelengths adapted from CD bands of anthracyclines in 0.05 M HEPES and 0.1 M KCl [35].

assumes at an internal pH of  $< 5.5$  (see Fig. 4IIA, IIC) within liposomes containing citrate and sulfate, respectively. Using CD analysis as a tool to evaluate doxorubicin, Fiallo et al. [27] have attempted to assign specific absorption bands to specific electronic transitions. These are summarized in Table 1 and suggest that absorption bands appearing at 330 and 346 nm wavelengths correspond to a  $n \rightarrow \pi^*$  transition at the C(12) position and a  $n \rightarrow \pi^*$  transition at the C(5) position. The results in Fig. 8C indicate an inverse of chirality at 330 nm for the citrate ( $\Delta\epsilon = -15.37$ ) and the  $MnSO_4$  plus A23187 ( $\Delta\epsilon = -6.94$ ) loaded liposomes as compared to doxorubicin encapsulated into the  $MnSO_4$  ( $\Delta\epsilon = 6.79$ ) loaded liposomes in the absence of ionophore. These results also indicate an inverse of chirality at 346 nm for the citrate ( $\Delta\epsilon = -9.51$ ) and the  $MnSO_4$  plus A23187 ( $\Delta\epsilon = -3.14$ ) loaded liposomes as compared to the spectra obtained for doxorubicin loaded into  $MnSO_4$  ( $\Delta\epsilon = 5.02$ ) liposomes without ionophore. En bloc, these observations strongly suggest that in the presence of  $Mn^{2+}$  and an internal pH of  $> 7.0$ , doxorubicin complexes with the metal ion, which interacts with the oxygen groups associated with the C(11)- $O^-$  and C(12)=O positions as well as the C(5)=O and C(6)- $O^-$  positions.

### 3.6. The influence of entrapped doxorubicin structure on drug release from liposomes in vitro and in vivo

The loading methods described provide effective means to prepare an encapsulated form of doxorubicin. The results also suggest that one can control the chemical and physical properties of the encapsulated drug by considering the use of an entrapped transition metal, such as  $Mn^{2+}$ , and a method whereby the drug-loaded liposome no longer exhibits a transmembrane pH gradient (pH 7.5 inside and out). From a practical point of view, however, it is critical to determine whether the loading methods used change drug release attributes in vitro and in vivo. These studies have focused, thus far, on liposomes prepared of DMPC/Chol, a lipid composition selected specifically because it is known that doxorubicin readily permeates across this lipid bilayer, as opposed to formulations prepared with DSPC/Chol, which retain drug for extended time periods both in vitro and in vivo. It is also important to recognize that others have indicated that formation of the doxorubicin citrate or  $SO_4$  precipitate as well as maintenance of a transmembrane pH

gradient (inside acid) are necessary if doxorubicin is to be well retained within a liposome following drug loading [7,18]. Therefore, it was anticipated that those formulations prepared in a manner that did not facilitate formation of the fibrous bundles and which resulted in substantial dissipation of the pH gradient would not be able to retain the entrapped doxorubicin. As shown in Fig. 9 (in vitro data) and Fig. 10 (in vivo data), this was not observed when the liposomal lipid composition was DMPC/Chol (55:45, mole ratio). For the in vitro assay, doxorubicin-loaded DMPC/Chol liposomes (0.2:1 drug-to-lipid ratio, wt/wt), were prepared using the citrate or the manganese-sulfate based loading procedures (with and without A23187), and diluted with fetal bovine serum and incubated at  $37^\circ C$  (Fig. 9). Changes in drug-to-lipid ratios, measured at various time points over a

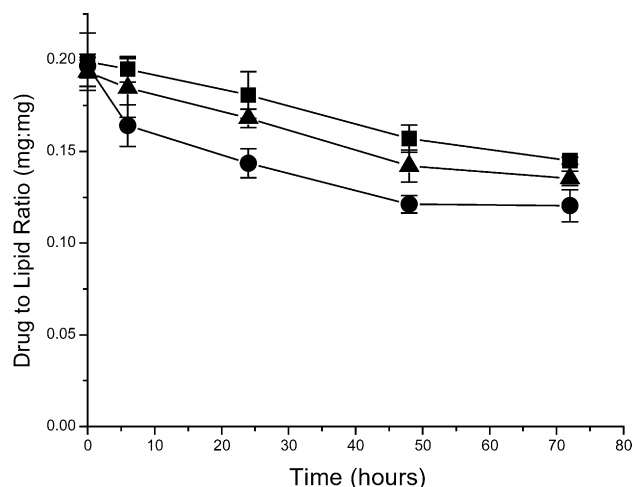


Fig. 9. The release of doxorubicin from DMPC/Chol (55:45) liposomes loaded using the procedures described in Fig. 2. Drug release was determined in vitro as described in Methods, where liposomes were loaded with doxorubicin to achieve a final drug-to-lipid ratio of 0.2:1 (wt/wt) using the citrate (■), the manganese sulfate (●), or the manganese sulfate loading procedure with the A23187 ionophore (▲). After drug encapsulation, each sample was mixed with fetal bovine serum (final serum concentration of 80% and lipid concentration of 2 mg/ml) and incubated at  $37^\circ C$ . At the indicated time points, the drug and liposomal lipid concentrations were measured after fractionating samples on a 1 ml spin column as described in Methods. These data were used to calculate a drug-to-lipid ratio at various time points. Data points represent the mean of data obtained from three separate experiments and the error bars indicate the standard deviation for each data point.

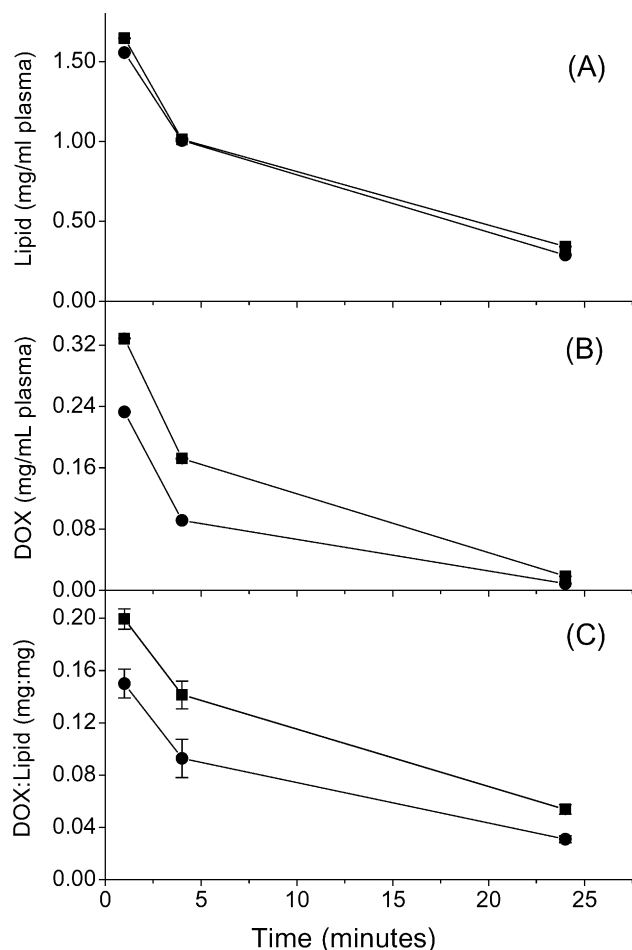


Fig. 10. The release of doxorubicin from DMPC/Chol (55:45) liposomes, following i.v. administration into female CD1 mice. Liposomes were loaded with drug to achieve a final drug-to-lipid ratio of 0.2:1 (wt/wt) using the citrate (■) or the manganese sulfate (●) procedures as previously described in Methods. Doxorubicin-loaded liposomes were adjusted to a concentration such that the lipid dose of 100 mg/kg could be administered in an injection volume of 200  $\mu$ l. At the indicated time points following injection, blood samples were obtained and plasma was prepared as described in Methods. Plasma lipid levels (A) were determined from measurements of <sup>3</sup>H-CHE as a liposomal lipid marker. The level of doxorubicin fluorescent equivalents (B) was measured in plasma using the drug extraction procedure described in Methods. The drug-to-lipid ratios (C) were calculated on the basis of the data shown in panels A and B. Each data point represents the mean drug-to-lipid ratio obtained from at least six mice and the error bars indicate the standard deviation of each data point.

72-h time course, indicated that all three formulations exhibit comparable drug release profiles. It can be suggested on the basis of these *in vitro* data, that more drug is released from the manganese sulfate-loaded liposomes prepared in the absence of A23187. This difference in drug release, however, can be accounted for by an observed 20% loss in encapsulated drug measured at the first time point (4 h after dilution into the serum-containing buffer).

Similar results were obtained *in vivo* following i.v. administration of the DMPC/Chol formulations (Fig. 10), where plasma elimination measurements for liposomal lipid

(Fig. 10A) and drug (Fig. 10B) can be used to calculate changes in drug release (Fig. 10C). These *in vivo* studies attempted to differentiate between the release of doxorubicin from DMPC/Chol liposomes where the drug exists as doxorubicin bundles (citrate loading technique) or a manganese complex (MnSO<sub>4</sub> procedure without A23187). Following i.v. injection in CD-1 mice (lipid dose of 100 mg/kg and drug dose of 20 mg/kg), measurements of plasma liposomal lipid levels (Fig. 10A) over 24 h indicated that the two formulations were eliminated from the plasma compartment at identical rates. Assessments of plasma doxorubicin levels (Fig. 10B) indicated that there were significantly lower levels of drug in the plasma at the 1 and 4 h time points when the drug was administered in the MnSO<sub>4</sub> liposomes loaded with drug in the absence of A23187 (two-tailed *P* values were <0.01 and 0.001, respectively). Consistent with the *in vitro* results, there was a rapid 20% loss of drug from these liposomal formulations within 1 h after administration. Subsequently, the rates of drug release from the two liposomal formulations were comparable (Fig. 10C). This result was unexpected considering that the two liposomal formulations exhibited remarkably different interior pHs; however, this result may just be a reflection of the increased permeability of the DMPC/Chol formulations. Under the time frame assessed, this formulation did not exhibit pH-dependent differences in drug release rates.

In order to demonstrate that drug release rates are dependent on liposomal lipid composition, the studies summarized in Fig. 10 were repeated for formulations prepared with DSPC/Chol liposomes. The loading attributes of the two different liposomal formulations were comparable in that >95% drug loading was achieved in within 10 min provided the liposomes were incubated with drug at 60 °C (results not shown). The results of this study are summar-

Table 2

Percent of encapsulated doxorubicin retained in liposomes following i.v. administration of DMPC/Chol and DSPC/Chol liposomes loaded with drug using encapsulated 300 mM citrate (pH 3.5) or the MnSO<sub>4</sub> method without the ionophore A23187<sup>a</sup>

Formulation	Time following administration <sup>b</sup>		
	1 h	4 h	24 h
DMPC/Chol–Citrate	100 ± 3.9 <sup>c</sup>	75 ± 5.5	27 ± 1.8
DMPC/Chol–MnSO <sub>4</sub>	100 ± 5.5	63 ± 7.3	21 ± 1.3
DSPC/Chol–Citrate	100 ± 5.4	95 ± 10.9	100 ± 3.8
DSPC/Chol–MnSO <sub>4</sub>	100 ± 6.4	73 ± 6.1	53 ± 3.5

<sup>a</sup> After drug loading, the latter formulations exhibited a transmembrane pH gradient of less than 0.5 units while the former exhibited pH gradients in excess of 3 units.

<sup>b</sup> As described in Fig. 10, following i.v. administration in CD1 mice, plasma concentrations of liposomal lipid and doxorubicin are measured at the indicated time points. These data are then used to calculate the drug-to-lipid ratio in the liposomes within the plasma compartment, a parameter that is used as a measure of *in vivo* drug release.

<sup>c</sup> The percent drug-to-lipid ratio was calculated using the measured drug-to-lipid ratio determined 1 h after administration as a value indicative of 100%.

ized in Table 2. Drug release attributes of the DMPC/Chol and DSPC/Chol formulations were estimated by calculating the percent change in the measured drug-to-lipid ratio determined at 1 h. As indicated by the data in Fig. 10C, the change in drug-to-lipid ratio determined for the DMPC/Chol formulations are comparable, regardless of whether the drug was encapsulated using the citrate-based methodology or the  $\text{MnSO}_4$  without ionophore. In contrast, results obtained with DSPC/Chol liposomes clearly demonstrate that the rate of drug release is more rapid when the drug is encapsulated using the  $\text{MnSO}_4$  (without ionophore) method. At the 24 h time point, liposomes prepared using this methodology exhibited a drug-to-lipid ratio of 0.09:1 (wt/wt) as compared to measured values of 0.18:1 (wt/wt) obtained for formulations prepared using the citrate method.

#### 4. Discussion

Doxorubicin has a broad spectrum of anticancer activity and is used to treat a variety of solid tumors as well as lymphomas and acute leukemias. One of many problems attributable to the use of this drug in its free form is its ability to engender cardiac toxicity, a toxicity that limits the amount of drug that can be given chronically [28,29]. Eliminating cardiotoxicity has been attempted with methods such as (1) alternative dosing [30], (2) pre/co-administration of free radical scavengers [31], (3) the development of semisynthetic derivatives [32,33] or (4) by liposomal encapsulation [34–36]. The latter approach provides a means of altering the biodistribution of drug whereby there are significant reductions in drug accumulation in cardiac tissues. There are now two liposomal–doxorubicin formulations approved for human use (Doxil™ or Caelyx™ and Myocet™). Despite the clinical development of this technology, there are still important questions to be addressed about the physical state of the entrapped drug. We believe that this information will be essential when considering the development of other liposomal anthracyclines as well as other drug classes.

Consistent with previous studies, the results presented here support the concept that drugs encapsulated in liposomes through use of ion gradients can form precipitates within the liposome. Our studies, however, clearly suggest that the nature of the entrapped precipitate is dependent on the internal pH and chemical composition. Importantly, these data also indicate that for a drug like doxorubicin, the resulting formulation can retain entrapped drug even under conditions where there is little or no residual pH gradient. Investigations focused on determining the factors controlling doxorubicin release from liposomes provide conflicting viewpoints. Certain studies indicate that high trapping efficiency, high drug-to-lipid ratios and stable drug retention are linked to the maintenance of a large pH gradient [7,13,37]. A reasoned explanation for these results was that as doxorubicin was encapsulated, the pH (inside) increased due to the consumption of protons as the neutral

drug became protonated. In turn, drug retention was thought to hinge on the equilibrium between the protonated and nonprotonated forms of doxorubicin. It was concluded that if a low interior pH were maintained, more doxorubicin would be in the protonated (charged) and thus in a membrane-impermeable state. In the case of liposomes prepared with DMPC/Chol, the *in vivo* release rates for preparations with and without a measurable pH gradient are essentially the same. For DSPC/Chol liposomes, there is a measurable change in the rate of drug release following *i.v.* administration, where drug release is greater for those formulations that lack a pH gradient. These observations would suggest that when liposomes are incubated at a temperature above the bulk phospholipid  $T_c$ , drug release occurs in a time frame that is not substantially influenced by the internal pH. Results obtained with DSPC/Chol liposomes, however, allow interior pH associated differences in *in vivo* drug release rates to be discerned. Perhaps most interesting, the methods described here provide a means to develop liposomal drug formulations where drug is encapsulated through very distinct mechanisms and chemical reactions.

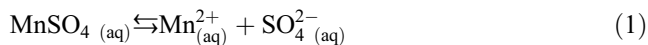
It has been well recognized by those using methods of drug loading that rely on ion gradients that drug accumulation levels often exceed that which would be predicted on the basis of ion redistribution according to the Henderson–Hasselbalch equation [7,9,13,25]. In the case of the anthracycline doxorubicin, these data have been explained by mechanisms involving membrane partitioning and/or drug precipitation [15–18]. It is well established, for example, that doxorubicin at concentrations of >30 mg/ml, in the presence of ammonium sulfate [15] or citrate [17], flocculates as a consequence of the formation of fibrous structures. cTEM studies indicated that the doxorubicin precipitate consisted of fibrous-bundle aggregates in both citrate- and sulfate-containing liposomes, with electron micrographs comparable to those shown here (Figs. 4). In terms of the physical state of doxorubicin, it has been proposed that the planar aromatic anthracycline rings stack longitudinally to form linear fibres within both citrate and sulfate-containing liposomes [16]. These fibres are aligned in a hexagonal arrangement to form bundles, with approximately 12–60 fibres per bundle. It was noted by these investigators that doxorubicin–citrate aggregates appear mostly as linear or curved structures (interfibre spacing was approximately 30–35 Å). Similarly, doxorubicin–sulfate aggregates are proposed to consist of rigid linear fibre bundles (interfibre spacing estimated to be approximately 27 Å). It was proposed that the sulfate anion, which is smaller than the citrate anion, might form a tighter packing arrangement resulting in decreased flexibility. As noted here under conditions where doxorubicin precipitates formed, the formulation containing citrate exhibited both curved and circular electron dense structures that caused a slight distortion of the liposome shape (Fig. 4IIA). In contrast, the sulfate-containing formulations exhibited primarily linear precipi-

itates and a significant elongation of the liposome (Fig. 4IIC). These differences in liposome shape appear to have little or no impact on the plasma liposomal lipid elimination profiles obtained following i.v. administration (see Fig. 10A).

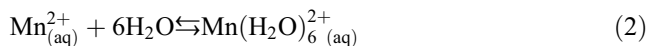
Our studies indicate that doxorubicin-loaded liposomes prepared using the  $\text{MnSO}_4$ - and  $\text{MnCl}_2$ -based procedures in the absence of A23187 are strikingly different than doxorubicin-loaded liposomes using the citrate procedure. Following drug loading, both of these formulations were a royal purple colour, as compared to the citrate-loaded preparations that are orange in appearance. Cryo-electron micrographs of the purple liposomal formulations indicated the appearance of an electron dense precipitate without any distinguishable crystalline structure. The resulting drug-loaded liposomes (prepared in the absence of A23187) also exhibited little or no transmembrane pH gradient. As shown in Figs. 9 and 10, these differences had little impact on drug retention attributes within the DMPC/Chol formulation but significant differences in drug release were observed for the DSPC/Chol formulation (Table 2). It was noted that on addition of the ionophore A23187 to these formulations, the encapsulated drug was in a form where it could readily assemble into fibre bundles, particularly in the  $\text{MnSO}_4$ -containing liposomes where addition of the ionophore generates a >2.5 unit pH gradient (inside acidic). Thus, the encapsulated drug is free to assume different chemical structures depending on the pH and the chemical composition within the liposomes.

Several studies have examined the role of transition metal anthracycline interactions [26,38,39]. These studies, which relied on a variety of spectroscopic methods, concluded that primary metal binding involved the deprotonation of the hydroxy anthraquinone moieties and the associated formation of a six-membered chelate. The absorbance spectra of doxorubicin in various concentrations of  $\text{MnSO}_4$  clearly showed a shift to higher wavelengths (lower energy). These absorption bands closely mimic those bands obtained following the deprotonation of doxorubicin at pH values above 10. Based on the spectroscopic information gathered from studies of multiple anthracycline derivatives [27,39], our data support the proposal that  $\text{Mn}^{2+}$  is interacting at both the C(11)  $\text{O}^-$  and C(12)=O positions and the C(5)=O and C(6)- $\text{O}^-$  positions. Other investigators looking at the binding of  $\text{Fe}^{2+}$  to anthracyclines have observed the deprotonation at the C(11)-OH and the C(6)-OH positions and the bathochromic shift from 480 to either 550–590 or 580–615 nm, respectively, for a variety of anthracycline derivatives including doxorubicin, pirarubicin, daunorubicin and idarubicin [39]. The strong CD band centred around 573 nm in the manganese doxorubicin-loaded liposome spectra confirms our belief that  $\text{Mn}^{2+}$  is complexed within these proposed coordination sites. Similar to the studies reported here, these investigators also reported that metal–anthracycline complexation resulted in a colour change from orange to blue-violet.

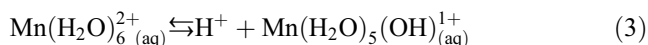
Complexation involving anthracyclines generally accompanies a theoretical increase of protons or a decrease in observed pH. This is not consistent with the results presented in Fig. 7, which clearly demonstrate that metal ion complexation does not result in formation of a pH gradient. It is suggested here that manganese complexes with doxorubicin in the following manner:



In water, the transition metal cations are always present as complex-hydrated ions;



The hydrated transition metal cations behave as weak acids in water,



$$K_a \text{ of } \text{Mn}(\text{H}_2\text{O})_6^{2+} \text{ (aq)} = 3 \times 10^{-11}$$

Because the hydrated manganese cation behaves as a weak acid and can dissociate to  $\text{Mn}(\text{H}_2\text{O})_5(\text{OH})_{\text{(aq)}}^{1+}$ , it most likely coordinates with the bidentate site offered by the C(11)-OH and C(12)=O positions or the C(5)=O and C(6)-OH positions neutralising the displaced hydrogen ion.

In summary, our studies have characterized the interactions between the transition metal manganese and doxorubicin, an interaction that promotes the accumulation of drug inside liposomes that contain this metal. The resulting drug-loaded liposome is unique in that the complexed drug is maintained in a form that is distinct from that identified for loading methods relying on maintenance of a pH gradient and formation of a citrate- or sulfate-based precipitate. The resulting liposomal drug formulation lacks a pH gradient, but still allows for effective drug retention attributes following i.v. administration. We are most excited, however, because the mechanism of drug loading occurs in a manner that is clearly distinct from methods involving use of pH gradients and it may be applicable to other drugs that possess coordination sites capable of complexing transition metals.

## Acknowledgements

We thank the staff of the Joint Animal Care Facility and the dedicated animal care staff of Advanced Therapeutics, and in particular Dana Masin and Rebecca Ng for all their help. We would also like to thank Norma Hudson and Linda Zhang for their assistance with the HPLC.

Funding for this research was supported by the Canadian Institutes of Health Research (M.B.B.), the Science Council GREAT Award and Celator Technologies Incorporated (S.A.A.).

## References

- [1] S. Paula, A.G. Volkov, A.N. Van Hoek, T.H. Haines, D.W. Deamer, *Biophys. J.* 70 (1996) 339–348.
- [2] D.D. Lasic, B. Ceh, M.C. Stuart, L. Guo, P.M. Frederik, Y. Barenholz, *Biochim. Biophys. Acta* 1239 (1995) 145–156.
- [3] T.E. Redelmeier, L.D. Mayer, K.F. Wong, M.B. Bally, P.R. Cullis, *Biophys. J.* 56 (1989) 385–393.
- [4] J.W. Nichols, D.W. Deamer, *Biochim. Biophys. Acta* 455 (1976) 269–271.
- [5] M. Bally, M. Hope, C. Van Echteld, P. Cullis, *Biochim. Biophys. Acta* 812 (1985) 66–76.
- [6] M.B. Bally, L.D. Mayer, H. Loughrey, T. Redelmeier, T.D. Madden, K. Wong, P.R. Harrigan, M.J. Hope, P.R. Cullis, *Chem. Phys. Lipids* 47 (1988) 97–107.
- [7] L.D. Mayer, L.C. Tai, M.B. Bally, G.N. Mitlenes, R.S. Ginsberg, P.R. Cullis, *Biochim. Biophys. Acta* 1025 (1990) 143–151.
- [8] L.D. Mayer, M.B. Bally, M.J. Hope, P.R. Cullis, *Biochim. Biophys. Acta* 816 (1985) 294–302.
- [9] T.D. Madden, P.R. Harrigan, L.C. Tai, M.B. Bally, L.D. Mayer, T.E. Redelmeier, H.C. Loughrey, C.P. Tilcock, L.W. Reinish, P.R. Cullis, *Chem. Phys. Lipids* 53 (1990) 37–46.
- [10] P.R. Harrigan, M.J. Hope, T.E. Redelmeier, P.R. Cullis, *Biophys. J.* 63 (1992) 1336–1345.
- [11] B.C. Cheung, T.H. Sun, J.M. Leenhouts, P.R. Cullis, *Biochim. Biophys. Acta* 1414 (1998) 205–216.
- [12] D.B. Fenske, K.F. Wong, E. Maurer, N. Maurer, J.M. Leenhouts, N. Boman, L. Amankwa, P.R. Cullis, *Biochim. Biophys. Acta* 1414 (1998) 188–204.
- [13] E. Maurer-Spurej, K.F. Wong, N. Maurer, D.B. Fenske, P.R. Cullis, *Biochim. Biophys. Acta* 1416 (1999) 1–10.
- [14] P.R. Cullis, M.J. Hope, M.B. Bally, T.D. Madden, L.D. Mayer, D.B. Fenske, *Biochim. Biophys. Acta* 1331 (1997) 187–211.
- [15] D.D. Lasic, P.M. Frederik, M.C. Stuart, Y. Barenholz, T.J. McIntosh, *FEBS Lett.* 312 (1992) 255–258.
- [16] D.D. Lasic, *Nature* 380 (1996) 561–562.
- [17] X. Li, D.J. Hirsh, D. Cabral-Lilly, A. Zirkel, S.M. Gruner, A.S. Janoff, W.R. Perkins, *Biochim. Biophys. Acta* 1415 (1998) 23–40.
- [18] X. Li, D. Cabral-Lilly, A.S. Janoff, W.R. Perkins, *J. Liposome Res.* 10 (2000) 15–27.
- [19] L.D. Mayer, M.J. Hope, P.R. Cullis, A.S. Janoff, *Biochim. Biophys. Acta* 817 (1985) 193–196.
- [20] C.H. Fiske, Y. Subbarow, *J. Biol. Chem.* 2 (1925) 375–395.
- [21] M.R. Niesman, G.G. Bacic, S.M. Wright, H.M. Swartz, R.L. Magin, *Invest. Radiol.* 25 (1990) 545–551.
- [22] G.L. Pool, M.E. French, R.A. Edwards, L. Huang, R.H. Lumb, *Lipids* 17 (1982) 448–452.
- [23] E. Wang, R.W. Taylor, D.R. Pfeiffer, *Biophys. J.* 75 (1998) 1244–1254.
- [24] M. Almgren, K. Edwards, G. Karlsson, *Colloids Surf.* 174 (2000) 3–21.
- [25] L.D. Mayer, M.B. Bally, P.R. Cullis, *Biochim. Biophys. Acta* 857 (1986) 123–126.
- [26] J. Bouma, J.H. Beijnen, A. Bult, W.J. Underberg, *Pharm. Weekbl., Sci.* 8 (1986) 109–133.
- [27] M.M. Fiallo, H. Tayeb, A. Suarato, A. Garnier-Suillerot, *J. Pharm. Sci.* 87 (1998) 967–975.
- [28] V.J. Ferrans, *Cancer Treat. Rep.* 62 (1978) 955–961.
- [29] D.D. Von Hoff, M. Rozenzweig, M. Piccart, *Semin. Oncol.* 9 (1982) 23–33.
- [30] D. de Valeriola, *Anticancer Res.* 14 (1994) 2307–2313.
- [31] A.R. Banks, T. Jones, T.H. Koch, R.D. Friedman, N.R. Bachur, *Cancer Chemother. Pharmacol.* 11 (1983) 91–93.
- [32] B.I. Sikic, M.N. Ehsan, W.G. Harker, *Science* 228 (1985) 1544–1546.
- [33] D. Platel, S. Bonoron-Adele, R.K. Dix, J. Robert, *Br. J. Cancer* 81 (1999) 24–27.
- [34] A. Rahman, A. Kessler, N. More, B. Sikic, G. Rowden, P. Woolley, P.S. Schein, *Cancer Res.* 40 (1980) 1532–1537.
- [35] A. Rahman, N. More, P.S. Schein, *Cancer Res.* 42 (1982) 1817–1825.
- [36] G. Batist, G. Ramakrishnan, C.S. Rao, A. Chandrasekharan, J. Gutheil, T. Guthrie, P. Shah, A. Khojasteh, M.K. Nair, K. Hoelzer, K. Tkaczuk, Y.C. Park, L.W. Lee, *J. Clin. Oncol.* 19 (2001) 1444–1454.
- [37] R.J. Lee, S. Wang, M.J. Turk, P.S. Low, *Biosci. Rep.* 18 (1998) 69–78.
- [38] F.T. Greenaway, J.C. Dadrowiak, *J. Inorg. Biochem.* 16 (1982) 91–107.
- [39] M.M. Fiallo, A. Garnier-Suillerot, B. Matzanke, H. Kozlowski, *J. Inorg. Biochem.* 75 (1999) 105–115.